ELSEVIER

Journal of Chromatography A, 815 (1998) 265–271

JOURNAL OF CHROMATOGRAPHY A

Short communication

Micromachined heated chemical reactor for pre-column derivatisation

Jan C.T. Eijkel[a], Albert Prak[b], Simon Cowen[c], Derek H. Craston[c], Andreas Manz[a,*]

[a]*Zeneca/SmithKline Beecham Centre for Analytical Sciences, Imperial College, London SW7 2AY, UK*

[b]*3T BV, P.O. Box 3639, 7500 DP Enschede, The Netherlands*

[c]*Laboratory of the Government Chemist, Queens Road, Teddington TW11 0LY, UK*

Received 13 February 1998; received in revised form 12 May 1998; accepted 20 May 1998

Abstract

A micromachined heated chemical reactor is presented. The microreactor consists of a sandwich of glass and silicon chips and contains a reactor channel of 50 μl volume. On-chip heating resistors supply a power of 2 W, resulting in a heating rate of 2°C/s. On-chip measuring resistors enable feed-back control of the temperature. The reactor volume makes the device suitable for derivatisation purposes in HPLC. As an example the pre-column derivatisation of amino acids with NBD-F is demonstrated, requiring 2 min of heating at 60°C, followed by HPLC separation and fluorescence detection.

Keywords: Microreactor; Derivatization, LC; Chip technology; Micro-total analysis system; Amino acids; 4-Fluoro-7-nitrobenzofuran; Sodium azide

1. Introduction

Pre- or post-column derivatisation is a very popular method to introduce or enhance detector sensitivity in liquid chromatography and electrophoresis [1]. For derivatisation reactions to proceed at an acceptable rate, the temperature must often be increased. For this purpose, the reaction mixture can be heated off-line or in a heated reactor. Heated reactors generally consist of a piece of PTFE tubing enclosed by a reservoir of heated water [1]. A disadvantage of such reactors is that they require a thermostatically controlled reservoir, which often means using a large and slowly reacting water bath. This paper presents the use of a micromachined heated chemical reactor, designed to provide a small, quickly reacting and low-power alternative. In the literature, examples can be found of micromachined reactors for chemical reactions [2], and for the polymerase chain reaction of DNA [3–6]. However, no work has yet appeared on micromachined heated reactors for derivatisation purposes.

The functioning of the reactor will be demonstrated by the pre-column derivatisation of five amino acids and subsequent separation on a HPLC column. The labelling agent is NBD-F (4-fluoro-7-nitrobenzofurazan, MW=183.1), a commercially available fluorigenic substance suitable for the derivatisation of primary and secondary amines [7]. After its introduction in 1981 by Imai and Watanabe [8], reports have been published on its use for pre-column labelling of amino acids [9–11] and a

*Corresponding author.

0021-9673/98/$19.00
PII: S0021-9673(98)00459-2

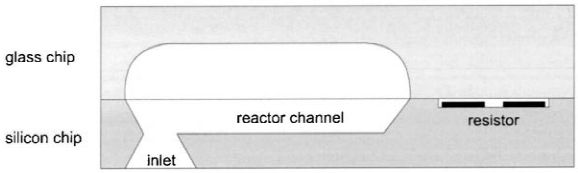

Fig. 1. Cross-sectional diagram of the reactor.

number of other amines [12] in the course of LC. The inset of Fig. 5 depicts the reaction with a primary amino acid. The reaction in 50% ethanol is complete after 1–5 min at 60–70°C at pH values around 8.0 [8]. The reaction products are stable at pH values below 5.0. An automated pre-column derivatisation procedure for amino-acids has been published [13].

2. Experimental

2.1. Reactor: description and fabrication

The reactor (see Figs. 1 and 2) was fabricated using silicon micromachining by 3T BV (Enschede, the Netherlands). It consists of a silicon bottom chip (thickness 0.4 mm) and a glass top chip (thickness 0.5 mm). The overall size of the reactor is 12×24×0.9 mm^3. The reactor chamber is formed by a 100 mm long and 1 mm wide, meander-shaped channel which is etched (33% KOH, 73°C) partly in the silicon (depth 200 μm) and partly in the glass (5% HF, room temperature) (depth 300 μm). The channel volume is 50 μl. Two through-holes in the silicon wafer (etched using 33% KOH at 73°C) serve as the fluid inlet and outlet. Prior to the etching of the

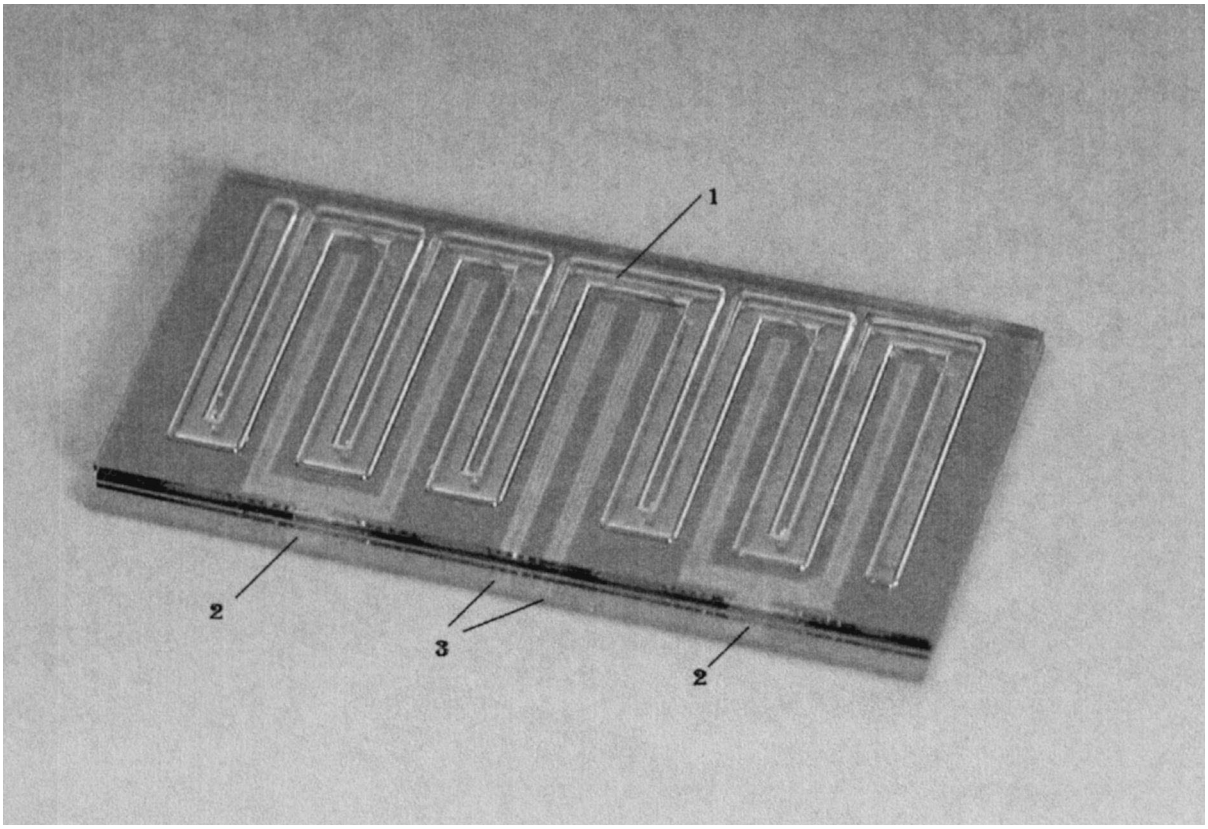

Fig. 2. Photograph of the reactor: 1. meander-shaped reaction channel; 2. Cr–Pt heating resistors; 3. Cr–Pt measuring resistors.

liquid channel, Cr–Pt thin film metal resistors were sputtered in a shallow groove (1.5 μm) in the silicon. The groove was produced by isotropic reactive ion etching (SF_6, N_2, 20 Pa). In this way the upper surface of the wafer remains flat for the glass bonding to be performed later. The metal pattern is isolated from the silicon by a thermal oxide (800 nm), grown by wet thermal oxidation at 1150°C. After completion of the processing, the silicon and glass wafers were assembled using anodic bonding. Finally, the wafers were cut into separate units. During the cutting, the pads for electrical contacts were exposed.

The temperature of the reactor can be raised up to a maximum of 90°C (depending on the thermal isolation of the reactor chip) by means of four Cr–Pt resistors of approx. 100 Ω (total power 2 W). The temperature is measured by the two temperature sensitive Cr–Pt resistors. All resistors are located in between the meanders, so that electrical contact with the liquid is not possible.

2.2. Apparatus

The reactor was glued onto a piece of circuit board using Silastic (Acetoxysilan) and in a later stage Sylgard 184 (silicone elastomer), both obtained from Dow Corning (Wiesbaden, Germany). Liquid contacts were made by extending two stainless steel pipes (length 6 mm and internal diameter 1 mm) through the circuit board to the through-holes in the silicon chip. The device was incorporated into the flow manifold schematically shown in Fig. 3. A Kloehn (Las Vegas, NV, USA) syringe pump with 5 ml syringe was used to transport the reaction mixture to the reactor and from there to the 20 μl injection loop of a model 7125 Rheodyne (Cotati, CA, USA) injection valve. All low-pressure connections were made with 0.8 mm ID PTFE tubing. A piece of tubing with an internal volume of 50 μl between the reactor and the injection valve was used for cooling the reaction mixture prior to injection. The reactor was shielded from direct light by aluminium foil. Between each measurement, the injection valve and the reactor were flushed three times with ethanol/water (50% v/v). Experiments were performed at room temperature (21–23°C).

The high-pressure part of the liquid system consisted of a Beckman 114M solvent delivery module with microflow liquid head (Beckman Instruments, Fullerton, CA, USA), the Rheodyne injection valve, a pre-column metal grid filter and an Alltech (Carnforth, UK) Econosphere C18 5 micron column, 150 mm×4.6 mm. Detection was performed using a

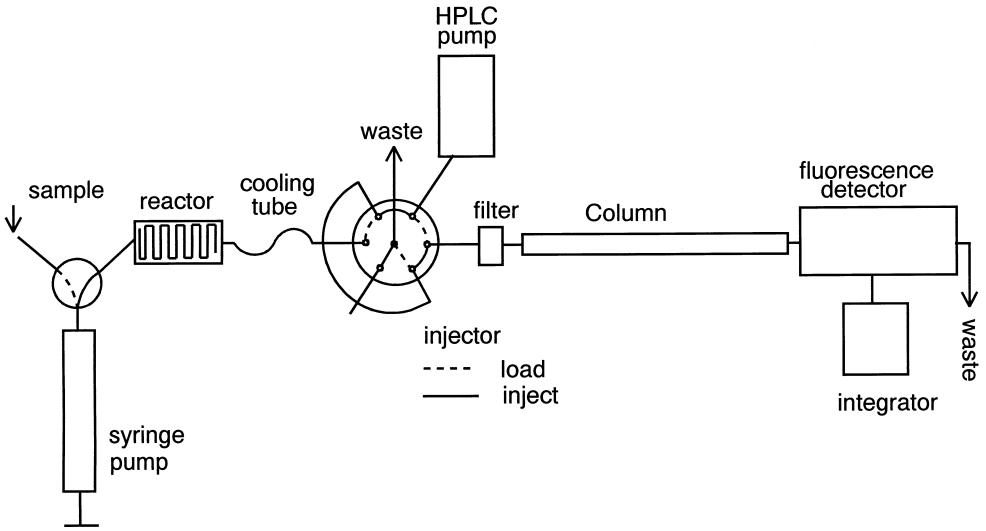

Fig. 3. Flow manifold.

Perkin Elmer LS-4 fluorescence spectrometer (λ_{ex} = 470 nm, λ_{em} = 540 nm) (Perkin-Elmer, Norwalk, CT, USA) and detection data were recorded by a Shimadzu C-R3A integrator (Shimadzu, Columbia, MD, USA).

The heating resistors of the reactor were powered by an Instek (City of Industry, CA, USA) PS-3030D DC power supply. The syringe pump and the Instek power supply were controlled using the PC serial port and an analog output channel of a PC-based AD-card (PCI-MIO-16-E-4, National Instruments, Austin, TX, USA), respectively. The measuring resistors were put in series and incorporated into a Wheatstone bridge circuit, using a battery for the driving voltage. The output voltage of the Wheatstone bridge was read into the PC and used in a feedback loop to control the chip temperature. All control was effected using a program written in Labview 4.0 (National Instruments).

2.3. Reagents

The amino acid solution contained 100 μ*M* of histidine, glycine, serine, citrulline and alanine in water. A 32 m*M* solution of NBD-F in ethanol was freshly prepared. A 50 m*M* borax buffer/ethanol solution was made by solving 953 mg of $Na_2B_4O_7.10H_2O$ in 50 ml of H_2O, adjusting to pH 7.8 with 3 *M* HCl, and adding 50 ml of ethanol. The mobile phase was 0.15 *M* phosphoric acid–acetonitrile (84:16, v/v) [14], and was degassed with He and filtered prior to use. All chemicals used were of analytical grade, the ethanol and acetonitrile were pro-HPLC grade. The water was purified using a Millipore Milli-Q50 installation. The amino acids were purchased from Sigma, St.Louis, MO, USA; the borax, ethanol, HCl and phosphoric acid from BDH chemicals Ltd., Poole, UK; the acetonitrile from Rathburn, Walkerburn, UK; the NBD-F from ICN, Costa Mesa, CA, USA.

2.4. Procedures

The reaction mixture was prepared in a vessel of brown glass by subsequent addition of 2.8 ml of buffer solution, 100 μl of the 10^{-4} *M* amino acid solution and 100 μl of the NBD-F solution. The mixture was immediately sucked into the syringe pump and 50 μl was injected into the pre-heated reactor. After 2 min at 60°C, the reacted mixture was transported into a 50 μl piece of tubing, where it was allowed to cool to room temperature for 1 min. Subsequently, it was transported into the 20 μl injection loop of the Rheodyne valve and immediately injected into the HPLC system. The applied flow-rate in the HPLC system was 1 ml min^{-1}.

For comparison of the heating procedure, the reaction mixture was heated for 2 min in a water bath, cooled in ice water and injected. A blank control was performed using a solution without amino acids. Its chromatogram showed only the peaks indicated as 5 and 6 in Fig. 5, probably belonging to NBD–OH and another side product. All peaks were identified by derivatisation and injection of the separate substances. The injection of only the ethanol-water mixture resulted in a small peak with a retention time of about 2 min.

3. Measurement results and discussion

3.1. Reactor characteristics

A typical reactor temperature curve is shown in Fig. 4. The reactor temperature increases with about 2°C per second in the pre-injection phase. On the injection of the reaction mixture, the temperature decreases temporarily and again on ejection of the reaction mixture. The oscillations between 58 and 62°C in the reaction phase are caused by the

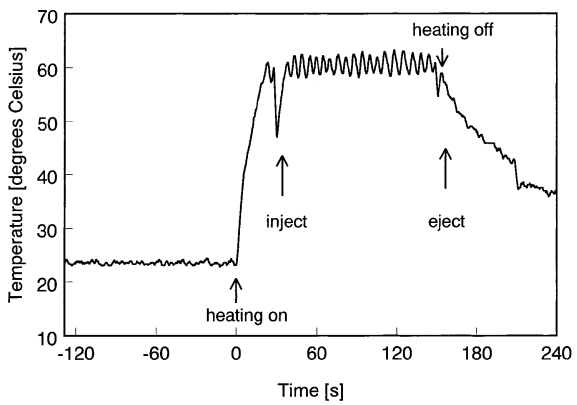

Fig. 4. Chip temperature curve. The moments of injection and ejection of the reaction mixture are indicated. E_g = 2 W.

temperature-controlled feedback loop. During heating, no visible air bubbles were formed in the reactor.

Some characteristics of the reactor can be deducted from the observed temperature curve. Under conditions for which temperature gradients within the solid are small, the lumped capacitance method can be used to describe the heating phase [15]. Such conditions will be shown to exist below. Following this method, the chip temperature, T, during the heating phase is described by

$$T = T_{\text{environ}} + \frac{E_g}{H}\left(1 - \exp\left[-\frac{H}{\sum \rho V c}\, t\right]\right),$$

where E_g is the generated heat [W], H the heat transfer to the environment per degree K[W K^{-1}], ρ the specific density [kg m^{-3}], c the specific heat capacity [J kg^{-1} K^{-1}] and V the volume [m^3]. The product of the last three terms ($\Sigma\rho Vc$) gives the heat capacity [J K^{-1}].

A fit of the equation to the 2W heating curve from 23 to 60°C results in $H = 0.046$ W K^{-1} and $\Sigma\rho Vc = 0.60$ J K^{-1}. The fitted value for the heat capacity is 0.2 J K^{-1} higher than the one calculated by summation of the heat capacities of the glass and silicon parts using the physical constants given in Table 1. This probably indicates a contribution of the printed circuit board and the stainless steel inlet and outlet pipes. The small heat capacity explains the observed rapid heating in 22 s.

It is important to assess if the measured temperature reflects the actual temperature of the reaction mixture in the liquid channel. The difference between both can be estimated from the time constants for heat transport on the chip.

We can define a time constant τ[s] for heat diffusion over a distance d in a medium with thermal conductivity λ[W K^{-1}m^{-1}], specific heat capacity c[J kg^{-1} K^{-1}] and density ρ[kg m^{-3}] as

$$\tau = \frac{c\rho d^2}{\lambda}$$

In the silicon bottom chip, the largest time constant equals 200 ms when calculated using this equation (for $d = 4.5$ mm, which is half the distance between two central heating resistors; see Fig. 2). This low value results from the excellent heat conduction in silicon. At $t = \tau$, 90% of the temperature difference will have disappeared [16]. This implies that the measured temperature constantly almost equals the temperature of the silicon near the liquid channels. During the measurements, even when the temperature increase is at its maximum of 2 K/s, the temperature difference in the silicon will always be less than 0.5 K.

Heat conduction in the water/ethanol reaction mixture is slower than in silicon. In the worst case, the reaction mixture will only be heated by the silicon underneath. The time constant then must thus be calculated for $d = 0.5$ mm (the channel height) and equals 2 s. At $t = \tau$, the average temperature in the channel will be 93% of the value in the silicon [16]. This implies that the reaction mixture takes some 2 s longer to heat to 60°C than is reflected by the measurements. Such a delay is negligible with respect to the total reaction time of 120 s. It can therefore be concluded that, for practical purposes, the measured temperature reflects the temperature of the reaction mixture. The time constant of 2 s also implies that the amplitude of the temperature oscillations in the reaction chamber is damped relative to the measured oscillations.

Table 1
Physical properties

	Thermal conductivity λ [W K^{-1} m^{-1}]	Density ρ [kg m^{-3}]	Specific heat capacity c [J kg^{-1} K^{-1}]	Volume V in reactor [m^3]
Si	148	$2.33 \cdot 10^3$	$0.70 \cdot 10^3$	$95 \cdot 10^{-9}$
SiO_2	1.2	$2.6 \cdot 10^3$	$0.75 \cdot 10^3$	$114 \cdot 10^{-9}$
Ethanol–H_2O (50:50, v/v)	0.41[a]	$0.93 \cdot 10^3$	$2.44 \cdot 10^3$[a]	$50 \cdot 10^{-9}$

[a] The averaged properties for 55.9% H_2O and 44.1% ethanol.

In the glass top chip, the largest time constant equals 1 s (for $d=0.8$ mm, which is the reactor channel height plus half its width). This implies that the glass also contributes to the heating of the water/ethanol mixture, decreasing the (worst-case) τ of 2 s calculated above. The three time constants of 200 ms, 1 s and 2 s justify the assumption of a homogeneous T during the heating phase, on which the use of the lumped-capacitance method was based.

3.2. Derivatisation

To optimise the derivatisation reaction in the present system, the heating temperature was varied between 50 and 70°C and the heating time between 1 and 4 min. Highest yields of reaction were seen at 60°C for 2 min. Fig. 5 shows a typical chromatogram of the NBD-F derivatives, with 67 pmol of every amino acid injected. The areas under the curve were about equal to the ones obtained when the reaction mixture was heated in a water bath at 60°C for 2 min. This result proves the adequate functioning of the reactor. The reproducibility of the procedure was also assessed. The coefficients of variation of the area under the curve with 67 pmol injected, using alanine as the internal standard ($n=7$) were for histidine 1.8%, glycine 0.8%, serine 1.0% and citrulline 1.4%. These values are acceptably low, reflecting the partial automation of the procedure. The detection limit ($S/N=3$) with the present set-up and reagent concentration was found to be about 500 fmol of the injected substances.

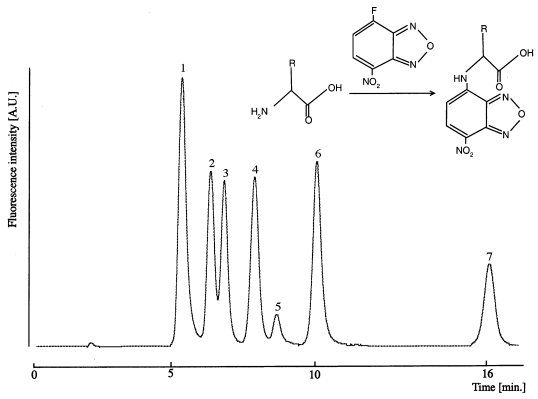

Fig. 5. Chromatogram of five derivatised amino acids. 1, NBD-histidine; 2, NBD- glycine; 3, NBD-serine; 4, NBD-citrulline; 5 and 6, NBD decomposition products; 7, NBD-alanine. Inset: The reaction of NBD-F with a primary amino acid to form a fluorescing product.

During the experiments it was discovered that the addition of 0.1% sodium azide to the amino acid mixture almost totally blocked the derivatisation reaction, while causing a large increase of peak 5. Apparently, sodium azide reacts with NBD-F or catalyses its hydrolysis. Azides should therefore not be used in solutions for NBD-F labelling.

4. Conclusions

The results show that the heated reactor can successfully be used for pre-column derivatisation. The device compares favourably with a thermostatically controlled water bath on the basis of its low volume ‘on the bench’. In addition, its power consumption is much lower and its heating rate more rapid. The typical power consumption for one derivatisation was only 180 J, and the heating rate 2°C s^{-1}. Its rapid heating and cooling rate will enable the execution of temperature programs with steep slopes. The device enabled an exactly timed heating procedure, leading to a low coefficient of variation between successive measurements. One of the possible applications of the microreactor is in an intelligent injection valve, through integration with the injection loop. Preferably, reagent mixing and injection must also be automated in such a valve. Another application would be as a flow-through reactor for post-column derivatisation, provided that excessive bandbroadening and increase of noise can be avoided. The reactor device could also be applied outside the HPLC area in places where low power consumption and versatile and rapid thermal programming are of importance. Finally, the device lends itself to future integration with suitable components for chip-based fluid-handling, separation and detection in a micro-TAS (micro-Total Analysis System) [17].

5. Acknowledgement

Elements of the work in this paper were supported under contract with the Department of Trade and

Industry as part of the Analytical Innovation Programme.

References

[1] I.S. Krull, Z. Deyl, H. Lingeman, J. Chromatogr. B 659 (1994) 1.
[2] W. Ehrfeld, V. Hessel, H. Lehr, in: A.Manz, H.Becker (Editors), Microsystem technology in chemistry and life sciences, Springer Verlag, Berlin, 1998, p. 233.
[3] A.T. Woolley, D. Hadley, P. Landre, A.J. de Mello, R.A. Mathies, M.A. Northrup, Anal.Chem. 68 (1996) 4081.
[4] J. Cheng, M.A. Shoffner, K.R. Mitchelson, L.J. Kricka, P. Wilding, J. Chromatogr. A 732 (1996) 151.
[5] M.A. Shoffner, J. Cheng, G.E. Hvichia, L.J. Kricka, P. Wilding, Nucleic Acids Res. 24 (1996) 375.
[6] J. Cheng, M.A. Shoffner, G.E. Hvichia, L.J. Kricka, P. Wilding, Nucleic Acids Res. 24 (1996) 380.
[7] K. Blau, J. Halket, Handbook of Derivatives for Chromatography, 2nd edition, Wiley, New York, 1993.
[8] K. Imai, Y. Watanabe, Anal. Chim. Acta 130 (1981) 377.
[9] Y. Watanabe, K. Imai, J. Chromatogr. 239 (1982) 723.
[10] Y. Watanabe, K. Imai, J. Chromatogr. 309 (1984) 279.
[11] M. Kato, T. Fukushima, T. Santa, H. Homma, K. Imai, Biomedical Chrom. 9 (1995) 193.
[12] K. Imai, S. Uzu, S. Kanda, W.R.G. Baeyens, Anal. Chim. Acta 290 (1994) 3.
[13] H. Kotaniguchi, M. Kawakatsu, T. Toyo'oka, K. Imai, J. Chromatogr. 420 (1987) 141.
[14] N. Watanabe, T. Toyo'oka, K. Imai, Biomed. Chromatogr. 2 (1987) 99.
[15] F.P. Incropera, D.P. DeWitt: Fundamentals of Heat and Mass Transfer, 4th edition, John Wiley and Sons, New York, 1975, pp. 212–213.
[16] H.S. Carslaw, J.C. Jaeger, Conduction of Heat in Solids, Clarendon Press, Oxford, UK, 1959, pp. 100–102.
[17] A. Manz, D.J. Harrison, E. Verpoorte, H.M. Widmer, in: Advances in Chromatography, Vol. 33, Marcel Dekker Inc., New York, 1993, pp. 1–66.